



University of Dundee

Visual programming for structural assessment of out-of-plane mechanisms in historic masonry structures

Funari, Marco Francesco; Spadea, Saverio; Lonetti, Paolo; Fabbrocino, Francesco ; Luciano, Raimondo

Published in:
Journal of Building Engineering

DOI:
[10.1016/j.jobe.2020.101425](https://doi.org/10.1016/j.jobe.2020.101425)

Publication date:
2020

Document Version
Peer reviewed version

[Link to publication in Discovery Research Portal](#)

Citation for published version (APA):

Funari, M. F., Spadea, S., Lonetti, P., Fabbrocino, F., & Luciano, R. (2020). Visual programming for structural assessment of out-of-plane mechanisms in historic masonry structures. *Journal of Building Engineering*, 31, 1-13. [101425]. <https://doi.org/10.1016/j.jobe.2020.101425>

General rights

Copyright and moral rights for the publications made accessible in Discovery Research Portal are retained by the authors and/or other copyright owners and it is a condition of accessing publications that users recognise and abide by the legal requirements associated with these rights.

- Users may download and print one copy of any publication from Discovery Research Portal for the purpose of private study or research.
- You may not further distribute the material or use it for any profit-making activity or commercial gain.
- You may freely distribute the URL identifying the publication in the public portal.

Take down policy

If you believe that this document breaches copyright please contact us providing details, and we will remove access to the work immediately and investigate your claim.

1 Visual programming for structural assessment of out-of-plane mechanisms in 2 historic masonry structures

3 Marco Francesco Funari*^{1,2}, Saverio Spadea¹, Paolo Lonetti², Francesco Fabbrocino³, Raimondo
4 Luciano⁴

5 ¹*School of Science and Engineering, University of Dundee, Nethergate, DD1 4HN, Dundee, United Kingdom*

6 ²*Department of Civil Engineering, University of Calabria, Via P. Bucci, Cubo39B, 87030, Rende (CS), Italy.*

7 ³*Department of Civil Engineering, Pegaso University, Napoli, Italy.*

8 ⁴*Department of Engineering, University of Naples Parthenope, Napoli, Italy.*

9 10 **ABSTRACT:**

11 This work aims at proposing a novel procedure for the seismic assessment of historic masonry
12 structures which is computationally efficient and does not rely on destructive material tests. Digital
13 datasets describing the geometric configuration of historic masonry structures are employed to
14 automatically generate a non-linear Finite Element (FE) model and investigate on possible collapse
15 modes. A configuration of failure surfaces is therefore detected through the Control Surface Method
16 (CSM), which is here proposed for the first time. In a following step of the analysis, structural
17 macroblocks are identified, whereas an upper bound limit analysis approach is employed to estimate
18 the structural capacity of the structure. Genetic Algorithms are also employed to detect the actual
19 failure mode for the structure. The procedure is implemented into a visual coding environment, which
20 allows one to parametrically explore all possible failure surfaces and immediately visualize the effects
21 of the user assumptions. This is particularly suited to support a decisions-making process which
22 strongly rely on engineering judgement. The procedure is validated by the analysis of several
23 benchmark cases, whose results are presented and discussed.

24

25 **Keywords: Masonry Structures; Pushover analysis; Upper bound limit analysis; Genetic**
26 **Algorithms; Visual Programming.**

27 **1. Introduction**

28 A considerable portion of the built environment is made of masonry, which represent a rich and
29 varied architectural heritage, especially in European countries [1]. Such ancient structures are
30 particularly sensitive to the effects of climate change, as recurrent freeze-thaw and wet-dry cycles
31 cause accelerated material deterioration and movement of foundations. However, the main cause of
32 damage to cultural heritage are earthquakes, which constantly cause heavy economic losses and
33 require difficult reconstruction processes [2, 3].

34 The assessment of the structural integrity of historical masonry structures is a challenging task,
35 mainly due to the inelastic and inhomogeneous mechanical response of the material. The existing
36 methods of analysis need a lot of computer power and detailed characterisation of the building
37 materials, which often must be partly destructive. However, they do not consider cracks and masonry
38 irregularities, which means that the results of such onerous analysis may be unreliable.

*corresponding Author: marcofrancesco.funari@unical.it

1 Additionally, historical masonry structures often present complex geometries and thus,
2 geometrical simplifications adopted at modelling stage may lead to either invalid or inaccurate
3 evaluations. Nowadays, modern survey techniques such as Digital Photogrammetry (DP) and 3D
4 Laser Scanning (LS) allow to quickly and accurately obtain all geometrical information needed [4-
5 8]. More challenging is converting large sets of information into a reliable and computationally
6 efficient structural model. In this context, Fortunato et al. [4] propose a strategy to obtain a Finite
7 Element (FE) model from very dense outlines, which are generated by point cloud slices. This
8 methodology is verified on an irregular structural geometry such as the Baptistery of San Giovanni
9 in Tumba (Italy). The limitation of this approach appears in the stage following the geometry
10 generation in which some defects of the Non-Uniform Rational Basis Spline (NURBS) model, such
11 as holes, self-intersection etc., are detected, as well in the need to fully characterise the non-linear
12 constitutive behaviour of masonry, which is here simplistically assumed as a homogenous. Castellazzi
13 et al. [5] develop an innovative refined strategy for the survey of historical masonry structures based
14 on LS or DP, in which the point cloud is transformed into a 3D FE model by means a semi-automatic
15 procedure. A similar work is proposed by Korumaz et al. [6], which employ LS data to build a CAD
16 based solid model.

17 Once defined the geometric model, different approaches might be used to assess seismic
18 vulnerability of masonry structures. D'altri et al. [9] identify two types of approach that are generally
19 adopted to assess the structural behaviour of masonry structures, these are either based on nonlinear
20 incremental or limit analysis methods.

21 Among incremental-iterative methods, nonlinear static analyses (or pushovers) assume a quasi-
22 static application of horizontal loads whilst taking into account for dynamic effects through a
23 simplified approach, whereas, non-linear dynamic analyses result in being computationally
24 demanding, as they requires a step-by-step integration in the time domain while explicitly considering
25 the dynamic nature of earthquakes. Moreover, both of these approaches require a rigorous modelling
26 of nonlinear material constitutive laws, in order to provide reliable results. Examples are the work
27 developed by Silva et al [10], which adopts a macro-modelling approach to assess seismic behaviour
28 of the structure by means pushover analysis with the distribution of forces proportional to the mass,
29 and Valente et al [11], which propose a numerical investigation based on the use of refined FE and a
30 nonlinear dynamic analysis for several historical masonry constructions.

31 Several are the drawbacks shown by these approaches. In addition to uncertainties due to the
32 material characterisation and the difficulty to model the non-homogeneous nature of masonry, it is
33 worth noting that historical structures generally show localized collapse mechanisms, which produce
34 convergence problems with consequent instability in the prediction of the actual load carrying

1 capacity. For these reasons, limit analysis is frequently used in civil engineering for a conservative
2 evaluation of the acceleration for the activation of the mechanism.

3 A limit analysis approach based on the upper bound theorem was proposed for the structural
4 assessment of structural behaviour of masonry structures for the first time by Heyman in his
5 revolutionary work [12], which has provided insight to several researchers [13-17]. According to
6 Heyman no-tension model, masonry is considered as a rigid, perfectly plastic material in compression
7 with no capability to resist tension. Limit analysis has the great advantage of being independent from
8 material properties but inevitably relies on a very simplified material model and results provided are
9 strongly dependent on the geometry of the failure surfaces considered. The upper bound method relies
10 on the search for the smallest load multiplier, while considering a number of collapse mechanisms
11 compatible with the structural restraint and the detected crack pattern [18]. To help with this, some
12 authors have already implemented algorithms able to find the most reasonable collapse mechanisms
13 into user defined routines of analysis [19, 20]. Fortunato et al. [19] develop a numerical procedure
14 for the limit analysis of 2D masonry structures subject to arbitrary loading. Similarly, in the
15 framework of limit analysis methods, other authors have proposed meta-heuristic approaches (i.e.
16 Genetic Algorithms) as a tool to explore the entity of loads associated with considered collapse
17 mechanism [21, 22]. Casapulla et al. [20], propose a simplified procedure for the prediction of the
18 collapse load and the failure mechanism of in-plane loaded masonry walls, assuming non-associative
19 frictional contact interfaces.

20 However, as reported by Giresini [23], preliminary global analyses are also able to provide
21 relevant information on possible collapse mechanisms, especially for structures are apparently in
22 good state of conservation and do not show any crack patterns. To this end, a new strategy based on
23 evaluating damage pattern obtained by non-linear dynamic analysis and the energy dissipated by each
24 macro-element during earthquakes was proposed in [18]. This procedure, based global/local
25 approach, suggests that the damage pattern identified by global analyses represent a good
26 approximation of the actual local or global collapse mechanisms. In this view, Cundari et al. [24]
27 have analysed structures with different numerical procedures, with the aim to detect the most likely
28 collapse mechanisms. Consequently, the upper bound limit analysis method is applied to analytically
29 compute the maximum horizontal acceleration the structure can withstand. Hence, the upper bound
30 limit analysis method is applied on the basis of the identified collapse mechanisms to analytically
31 compute the maximum horizontal acceleration that could be applied to the building. Similarly, Betti
32 et al. [25] investigate the seismic vulnerability of an historical construction by combining a global
33 pushover analysis with a simplified approach based on the kinematic method. Mele et al. [26] and
34 Brandonisio et al.[27], have developed a two step analysis. In the first step, the structure is analysed

1 in the linear-elastic range by using a 3D FE model. Subsequently, a pushover analysis of the single
2 macro-elements is performed. The results obtained through push-over analysis are compared to the
3 collapse loads derived from limit analysis, proving the ability of finite element nonlinear model to
4 provide reliable simulations of the actual response of masonry elements. Mendes et al. [28] have
5 devoted their work at evaluating the out-of-plane response of historical masonry structures. They
6 employ a FE modelling based pushover analysis which embeds a simplified micro-modelling
7 approach to detect the out-of-planes mechanisms. The maximum load capacity is estimated using the
8 upper bound method of limit analysis. Similarly, Foti et al. [29, 30] developed pushover analyses in
9 order to investigate the behaviour of trilitic large blocks in simple masonry structures.

10 The main aim of the present research is to develop a method for the rapid assessment of masonry
11 structures by combining concepts arising from non-linear continuum modelling, limit analyses
12 theorem and evolutionary solvers. The workflow is all integrated into a visual program implemented
13 into the environment offered by Rhinoceros3D+Grassoppher, which allows to parametric handle a
14 large set of information through object-oriented scripts. This is particularly suited to establish how
15 complex geometries can influence the mechanical response of materials and structures. Furthermore,
16 it allows to immediately visualise the effect of the user assumptions, allowing to integrate parametric
17 modelling into decisions-making processes which relays on engineering judgement.

18 The digital tool can manage the data arising by either non-linear static or dynamic analyses to
19 detect the most likely collapse mechanism through the proposed Control Surface Method (CSM),
20 which is here proposed for the first time. Based on such failure surfaces, Genetic Algorithms are used
21 to generate other possible collapse mechanisms and search for the actual failure mode corresponding
22 to the minimum value of the load multiplier. The paper is organized as follows. Section 2 describes
23 the method of analysis. Section 3 illustrates the implementation of the proposed procedure by means
24 the visual programming language. Section 4 reports a validation example and the investigation on a
25 benchmark case of study. Finally, some remarkable conclusions are discussed in Section 5.

26

27 **2. Method of Analysis**

28 Existing codes available from the literature, such as the Eurocode 6 [31], as well as the Italian
29 NTC 2018 [32] and Guidelines for the built heritage [33], suggest to perform static or dynamic non-
30 linear analyses to assess the seismic performance of these structures. Typically, static non-linear
31 analysis (pushover methodology) is utilized as it is certainly computationally more efficient. This is
32 based on the use of capacity curves expressed in terms of base shear and displacement of the control
33 point. On the basis of the capacity curve, the structural integrity is identified by using N2 method,
34 which was proposed by Fajfar [34] for framed structures, and subsequently extended to historical

1 masonry buildings [35-37]. As reported in [38, 39], the evaluation of the collapse acceleration, which
 2 activates the mechanisms, strongly depends on the choice of the control point. Choosing a control
 3 point rather than another one, might produce erroneous structural assessment especially for
 4 irregular structures, which cannot guarantee a box behaviour.

5 In order to overcome this issue, a new method of analyses is here proposed. The algorithm relies
 6 on the results arising from a global analysis to detect a first approximation of the macro-block
 7 geometry affected by out of plane mechanisms. This is used to perform an evaluation of the seismic
 8 vulnerability of the masonry structure on the basis of the upper bound method of limit analysis. This
 9 procedure is embedded into a visual program to allow the user to parametrically explore and visualise
 10 the collapse mechanism under investigation.

11 It is assumed that a refined geometric model of the structural problem is available, whereas
 12 assumptions are made on mechanical properties of constituent material in absence of detailed
 13 information. The first step of the proposed procedure consists of a global non-linear static analysis of
 14 the masonry structure. During the numerical simulation, the displacements of several control points,
 15 a priori selected on the top of the structures, are detected and stored.

16 In the present procedure, this information is employed to construct a three-dimensional surface,
 17 named hereafter Control Surface (CS), by interpolating the displacement function obtained during
 18 the step-by-step global analysis of all control points. Figure 1 refers to a multi-story masonry building
 19 considered as benchmark example in this work that will be described in detail in section 4. The CS
 20 arising from a non-linear static analysis is reported. Here the control points are identified by a two-
 21 variable curve featuring the X and Y coordinates corresponding the real position in the XY plane,
 22 whereas the function $Z(X,Y,i)$ represents the horizontal displacement occurred during the step-by-
 23 step global analysis, function of the X,Y coordinates as well as the (*i*-th) step in the loading history.

24 Among the CS generated at different load increments, the one corresponding to the maximum
 25 displacement is taken into consideration:

$$26 \quad f(X,Y) = \max[\|u\|]. \quad (1)$$

27 which, in principle, corresponds to the last load increment.

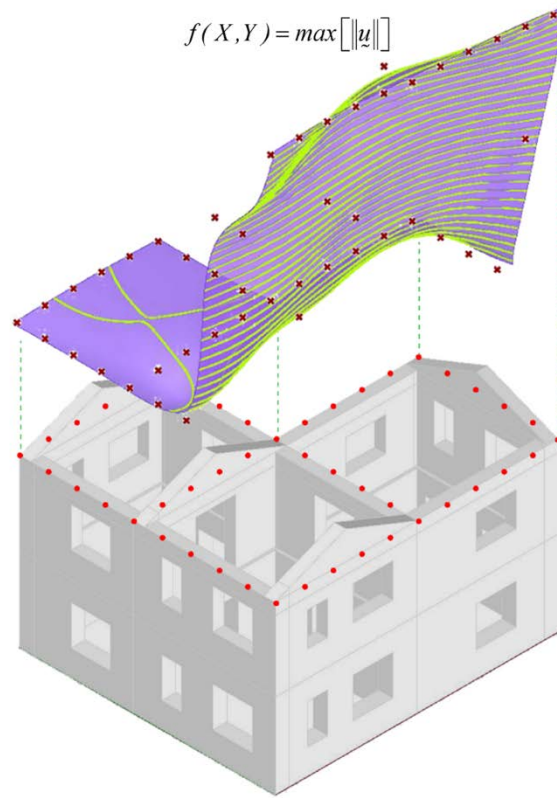
28 For the analytical surface $f(X,Y)$, the slope is computed as the gradient vector of the function:

$$29 \quad \nabla f(X,Y) = \left[\frac{\partial f}{\partial X}, \frac{\partial f}{\partial Y} \right]. \quad (2)$$

30 Hence, in order to represent a slope map, the norm of the CS is computed as:

$$31 \quad \|\nabla f(X,Y)\| = \sqrt{\left(\frac{\partial f}{\partial X}\right)^2 + \left(\frac{\partial f}{\partial Y}\right)^2}. \quad (3)$$

1 This formula is not based on a rise-over-run calculation over a fixed interval, but rather assumes
2 that a plane surface tangent to $f(X, Y)$ exist at any point of the surface. This is closely related to the
3 concept of Euclidean distance, and simply shows how much the surface f rises with a small fixed
4 increment in X and Y .



5

6

Figure 1: Control Surface detected at last loading increment of the non-linear static analysis.

7

8

9

10

11

12

13

14

15

16

17

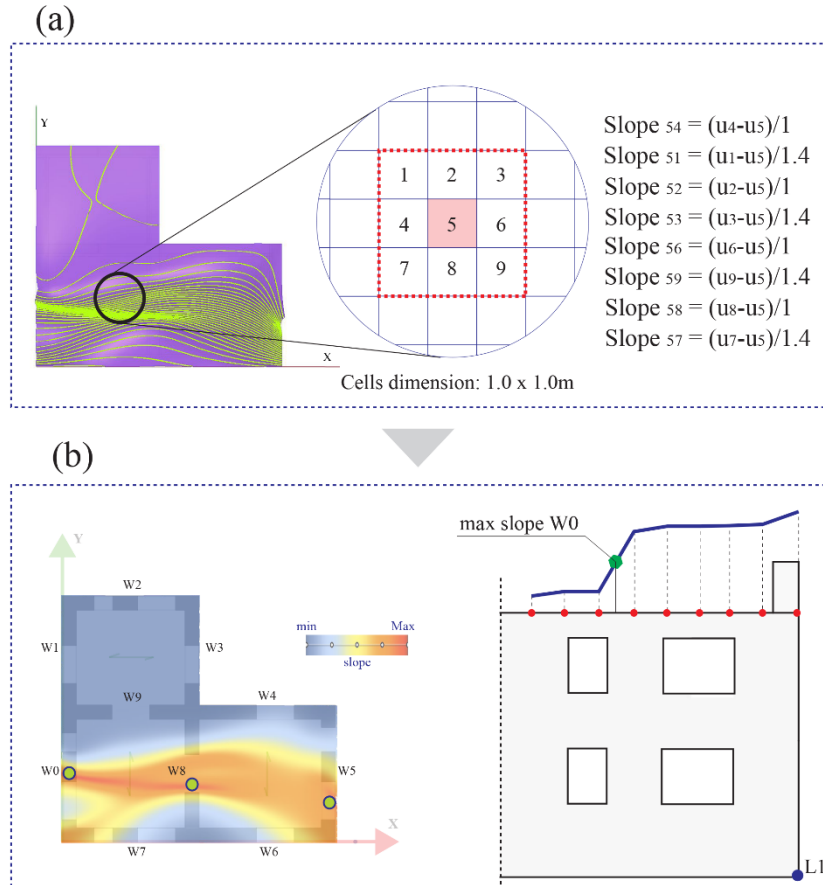
18

In order to perform the slope analysis, computational steps typically adopted in Geographic Information System (GIS) analysis are implemented. Once that the CS is built, this is discretized by using a refined quadrangular mesh (Figure 2a). For each of the resulting cell, the gradient of the eight adjacent cells is computed, assuming that the distance between two adjacent centres of the cells depend on the basis of the direction. Consequently, the computation of the slope is carried out by evaluating the gradient of $f(X, Y)$ between a cell and its eight adjacent (3x3 floating window). Finally, as shown in Figure 2b, the maximum value is stored, and it is used to represent the slope map.

It is worth noting that the procedure described above is integrated by a “local analysis” performed on the selected walls of the structure. Once the slope maps are plotted, the user can visually identify the wall where the maximum slope value is obtained. Figure 2b shows that higher values of the slope result in correspondence of the walls W0, W8 and W5, which are selected and analysed separately in

1 order to define the cutting planes. The walls W7 and W8 are involved in the overturning mechanism,
 2 thus exhibit an approximately constant value of the coordinate Z of the CS

3 On the right of the Figure 2b a representation of the local analysis of the side wall is reported.
 4 From the mechanical point of view, the slope value is proportional to the medium strain which occurs
 5 between two control points.



6
 7

Figure 2: Slope map representation and local analysis performed on single sidewalls.

8 As shown in Figure 2b, the slope map provides a representation of the region in which the
 9 displacements gradient is obtained from the pushover analysis. The synoptic meaning of the CS is to
 10 provide an easily understating representation of the weak regions identified by using a global analysis.
 11 Indeed, by considering the part of structures below the higher slope region of the CS, it is possible to
 12 identify the part of structures affected by local failure phenomena. The control surface is consequently
 13 allowing the user to define the macroblocks system and the appropriate location for the cylindrical
 14 hinge that is going to determine an out-of-plane mechanism. Figure 3 shows the geometry of the
 15 macro-blocks and the displacement map arising from the nonlinear static analysis at the final
 16 incremental load step.

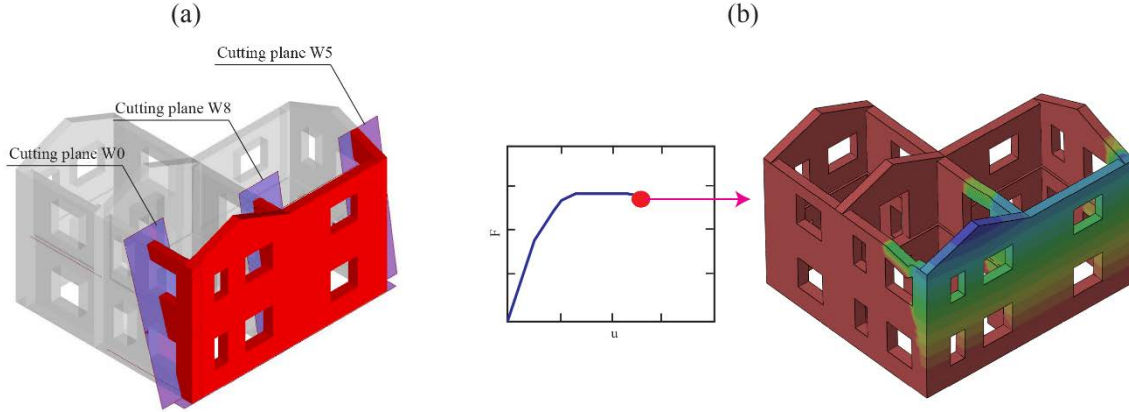


Figure 3: (a) Geometry of the macro-block obtained from the visual program; (b) Displacement map arising from the non-linear static analysis at the last load increment.

Once the geometry of the macro-block involved in the mechanism is defined, the appropriate distribution of loads are applied and the maximum load multiplier causing the failure of the structure, α_0 , is detected by using the upper bound theorem of the limit analysis, also taking into account the frictional behaviour at contact interfaces [40].

The computation of α_0 is therefore performed using the virtual work principle:

$$\alpha_0 \sum_{i=1}^n W_i \delta_{(x,y),i} - \sum_{i=1}^n W_i \delta_{(z),i} - \sum_{s=1}^n F_{f,s} \delta_{(z),s} = 0 \quad (4)$$

where W_i are the inertia forces arising from floors and roofs as well as the self-weights of the masonry walls, whereas $F_{f,s}$ are the frictional forces computed under the hypothesis of maximum frictional resistance for each sidewall. A discussion about the choice of the friction coefficient as well as its physical meaning for sliding rocking failure is neglected, However, this is extensively deepen in the works developed by other authors [16, 40], which largely adopt the hypothesis of dry-joint, which is valid in case of very weak mortar. It is the opinion of the authors that operating under this hypothesis is particularly appropriate when dealing with ancient buildings, where mortar joints may result particularly deteriorated.

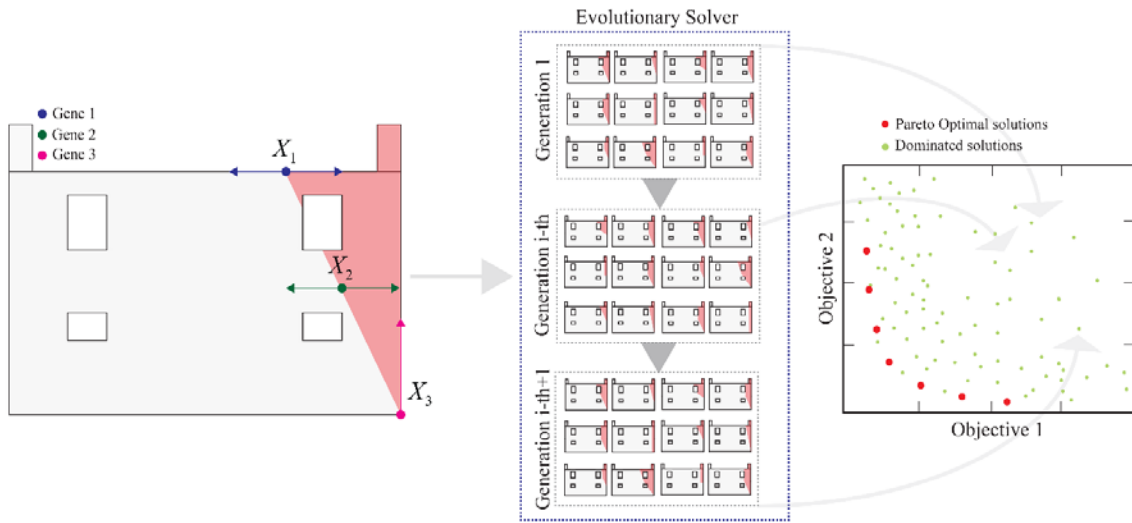
As already mentioned, the collapse mechanism detected needs to be further considered in order to guarantee the kinematically compatible load factor (determined through the upper bound method) is also statically determinate. To this end, an iterative procedure aims at refining the geometry of the macro-block. The minimum load factor capable to activate the overturning mechanism is therefore computed through an optimisation routine, while varying the position of the points that discretize the cracked surface. As shown in Figure 4, the position of the points X1 and X2, which represent the optimization variables, discretize the cracks line. Their abscissa can vary into a length range that is set equal to the distance between two pushover's control points previously mentioned. Thus, the

1 solution of this optimization problem is obtained by solving the following constrain minimization
 2 problem:

$$3 \quad \begin{cases} \text{minimize} : \alpha_0 \\ \text{subject to} : \sum_1^n F_h^i = 0 \end{cases} \quad (5)$$

4 where α_0 is the load multiplier and F_h^i is the i -th horizontal force.

5 According to [40], the optimization problem has to be solved by considering the horizontal
 6 equilibrium as a constraint. To this end the proposed methodology utilise an Evolutionary Solver (ES)
 7 in order to research a solution to the constrained optimization problem reported in Eq.(5).



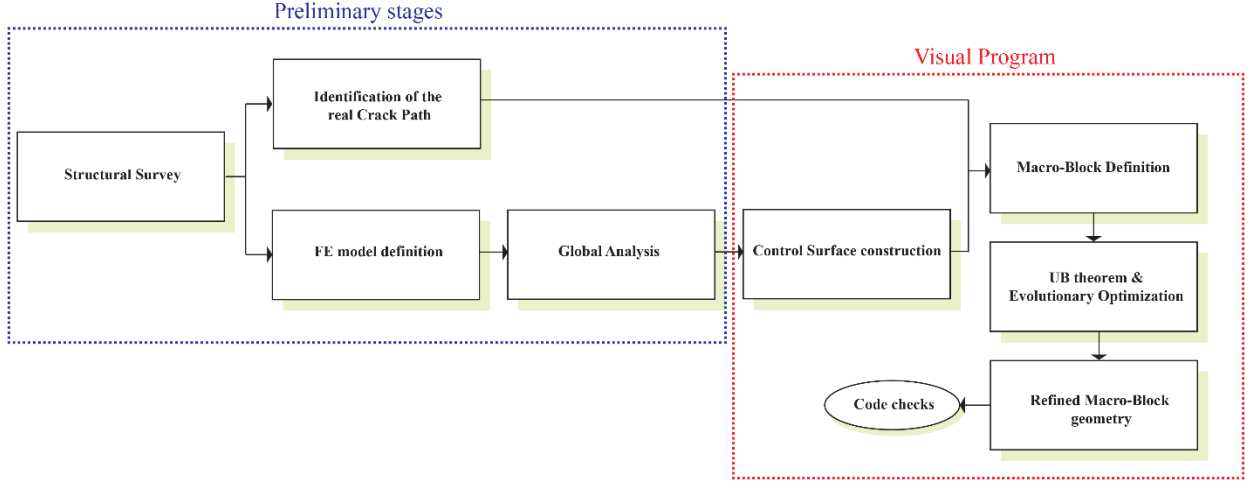
8
 9 *Figure 4: Evolutionary Solver: Genes definition, generations representation and graphical representation of the genomes.*

10 ES uses the same techniques such as reproduction, mutation, selection and recombination.
 11 According to biological vocabulary, the variables which are allowed to change are called genes.
 12 Basically, as the i -th gene changes, the state of the model changes and it either becomes better or
 13 worse (depending on what the user is searching for). Initially, a population composed of randomized
 14 genes (dimension values) is generated and by assessing the fitness of each chromosome (permutation
 15 of genes), the initial landscape points of the search space are identified. New populations of
 16 chromosomes are then generated based upon parent selection, crossover and mutation, and the fitness
 17 reassessed until the required conditions are found [41].

18 According to [16], once found the macro block geometry which satisfies Eq. (5), the visual
 19 program computes the kinematically compatible load factor corresponding to the same macro block
 20 geometry, but based on the hypothesis of nil activation of frictional resistances along the same cracks.

21 Furthermore, the capabilities of the proposed procedure might be improved by introducing
 22 computational steps devoted to perform the code checks prescribed by the code NTC 2018 [32] and

1 the Guidelines for the built heritage [33]. A synoptic representation of the algorithm is reported in
 2 Figure 5.



3
 4 *Figure 5: Schematic representation of the proposed procedure.*

5 6 **3. Numerical Implementation**

7 **3.1 A preparatory step: non-linear static analysis**

8 As mentioned above, the first stage of the proposed procedure is based on the analysis of the global
 9 structural behaviour, which is carried out through a non-linear static analysis. This step can be
 10 implemented into a general purpose nonlinear FE software. For the purpose of this paper, the
 11 geometrical model is imported into Abaqus CAE [42], and discretized into 3D tetrahedral elements
 12 with linear interpolation functions. The non-linear constitutive behaviour of masonry material is taken
 13 into account using the Concrete Damage Plasticity (CDP) material model which is embedded in the
 14 software [43], whose parameters are set in order to simulate the behaviour of historic masonry. The
 15 CDP assumes a scalar isotropic damage with different damage description in tension and in
 16 compression. The damage variables (d_c and d_t) are adopted to reduce the initial elastic modulus by
 17 means of the following standard relationships:

$$\begin{aligned}
 \sigma_c &= (1 - d_c) E_0 (\varepsilon_c - \varepsilon_c^{pl}) \\
 \sigma_t &= (1 - d_t) E_0 (\varepsilon_t - \varepsilon_t^{pl})
 \end{aligned}
 \tag{6}$$

18
 19 where σ_t and σ_c are the mono-axial tensile and compressive stress, E_0 is the initial elastic modulus,
 20 ε_t and ε_c are the total strain in tension and in compression, ε_t^{pl} and ε_c^{pl} are the equivalent plastic
 21 strain in tension and in compression. As extensively reported in literature [44], the compressive
 22 strength is normally playing a minor role in masonry collapse, as masonry capability to redistribute
 23 stresses reduce the occurrence of relevant crushing phenomena. Different is the case of tensile
 24 stresses, which are always associated with severe cracking and modification of the material

1 properties. It is therefore assumed in this model that the damage to occur in tension, i.e. a reduction
2 of the material strength and stiffness is applied in case of principal stress exceeding the maximum
3 admissible tensile strength.

4 The CDP model uses a Drucker-Prager strength criterion, modified through a parameter, K_c , which
5 represents the ratio between the distance from the hydrostatic axis of the maximum compression and
6 tensile stress. Furthermore, the CDP model considers an eccentricity parameter, which is able to
7 regularize the tensile corner, and a non-associated potential flow rule for the elasto-plastic
8 deformation part.

9 It is worth highlighting that such analysis is preparatory for the next steps and can be performed
10 according to several approaches. The user has complete freedom to choose the most appropriate finite
11 elements and mesh to discretize the geometric model as well as the constitutive law to take into
12 account for material nonlinearity [45]. As this remains a preliminary step, only needed to provide an
13 estimate of the collapse modes of the structure, the mechanical properties employed are not supposed
14 to strongly influence of the actual assessment of the structural capacity, which is to be performed in
15 a following step.

16

17 **3.2 Digital tool for the assessment of out-of-plane collapse mechanisms**

18 Results from nonlinear analysis are linked to the computational tool for the assessment of out-of-
19 plane collapse mechanism implemented in the visual programming environment offered by
20 Rhinoceros3D+Grasshopper. The developed algorithm has been compartmentalized into numbered
21 clusters, where each cluster performs a logical function in the global generation of the solution.

22 The first step of the visual algorithm consists of generating the geometric model of the case study
23 under analysis. Because of the shape complexities featured by historical masonry constructions, the
24 geometrical modelling is a fundamental task to assess their structural performance. Although the
25 geometric definition of the 3D model is out of the scope of this work, this must respond to the
26 following features: all vertical components are to be modelled as solid elements; floors and roofs are
27 not to be embedded in the model, while the actions associated with them and acting on vertical loads
28 are modelled as a uniform line load.

29 The second step consists of constructing the CS as according to the procedure described in Section
30 2. Each control point pertains to its own cluster which is used to both manage and visualize the point.

31 Control points are grouped into a list, which is adopted to define the surface through the procedure
32 described above. As shown in Figure 1: Control Surface detected at last loading increment of the non-
33 linear static analysis., the CS is represented through a contour map, which allows to graphically

1 visualize the regions where the CS surface slope is higher, i.e. the regions exhibiting the maximum
2 relative displacements.

3 In order to apply the upper bound method of the limit analysis, the definition of the macro block
4 geometry is required. To this end, the data provided by the CS are adopted to define the failure surface
5 which define the portion of structure affected by the local mechanism. This routine of the visual
6 program can run automatically, whilst the user has the faculty to interact and influence the positioning
7 of a cylindrical rotation hinge. The user can also define the discretisation of the failure surface and
8 consequently increase the number of control points. Each single node is connected to independent
9 slider which varies on a range set on the basis of physical assumptions. As the position of the control
10 points assume the meaning of genes in the evolutionary solver process (Figure 4), this decision
11 strongly affects the computational efficiency of the algorithm

12 In order to compute the horizontal acceleration needed for the activation of the local mechanism
13 of collapse, a fundamental prerequisite is the definition of the load acting on the macro block
14 previously detected.

15 The self-weight of the block is applied to its gravitational centroid, whereas the actions due to
16 floors as well as roofs are assumed as uniform line loads. Thus, the proposed algorithm is able to take
17 into account both the masonry self-weight and additional actions arising from the floors or the roofs.
18 the self-weight is automatically defined by introducing the specific gravity of the masonry (green
19 rectangle), and consequently applied to the volume of the macro-elements. The outputs of this cluster
20 are therefore the structural self-weight as well as the lever arm between the macro-elements centroid
21 and the cylindrical rotation hinge.

22 The user needs to draw a line corresponding to the floor or roof support and to introduce the weight
23 per unit length. Thus, the outputs of the cluster consist of the total weight acting on the block as well
24 as the horizontal and vertical distance of its application point from the cylindrical rotation hinge.

25 26 **3.2.1 Upper bound method of limit analysis and Evolutionary Solver**

27 The core of the visual code is devoted to compute the load multiplier that generates the activation
28 of the mechanism. According to the procedure developed by Casapulla et al. [16], this is computed
29 under the assumption of the maximum frictional resistance.

30 With the aim to compute the minimum of the upper-bound load multipliers which guarantees the
31 horizontal equilibrium, an evolutionary solver is adopted. The geometry of the failure surfaces is
32 parametrized by means of a set of sliders that vary on a range set by the user. In the spirit of
33 evolutionary algorithms, the solver iteratively modifies a population of individual solutions. During
34 each iteration, the solver randomly selects individuals from the current population and uses them as

1 parents to produce the children for the next generation. For each iteration, the population “evolves”
2 until an optimal solution is found.

3 The minimization problem reported in Eq. (5), can be numerically solved as a multi-fitness
4 problem which minimizes α_0 and satisfies the equilibrium of horizontal forces, concurrently.
5 Accordingly, the octopus component minimize the acceleration for the activation of the mechanism,
6 which guarantees the horizontal equilibrium (first fitness function) [16], by modifying the failure
7 surface of the masonry structure in the 3D space and, consequently, the geometry of the macroblock
8 considered for the equilibrium (second fitness function).

9 The same solution can be achieved using different optimization tools. In the present study, the
10 solution process is also performed by using Nelder-Mead Optimisation (NMO) component [46]
11 which is based on the Nelder-Mead method, a local search-based optimisation algorithm..

12 According to the procedure proposed in [16], once found the macro block geometry which satisfies
13 Eq. (5), the visual program computes the kinematic load factor, α_{upp} . An additional load multiplier,
14 α_{low} , is computed under the hypothesis of nil frictional resistance along the cracks. This certainly
15 represents a conservative solution that may be appropriately employed to perform code checks.

16

17 **4. Results**

18 In this section the limit analysis methodology (red rectangle in Figure 5) is validated on a
19 benchmark case study available in literature [20]. Furthermore, the whole assessment procedure (blue
20 and red rectangle in Figure 5) is applied to a multi-stores masonry building with irregular shape in
21 plane.

22

23 **4.1 Validation example**

24 A masonry wall loaded in his plane is here considered to validate the suitability of the proposed
25 procedure to solve the minimization problem described in Eq. (5). Figure 6 shows the geometry of
26 the case study, which consist of an assemblage of bricks subjected to in-plane horizontal forces. In
27 the present example a friction coefficient equal to 0.65 is considered [20].

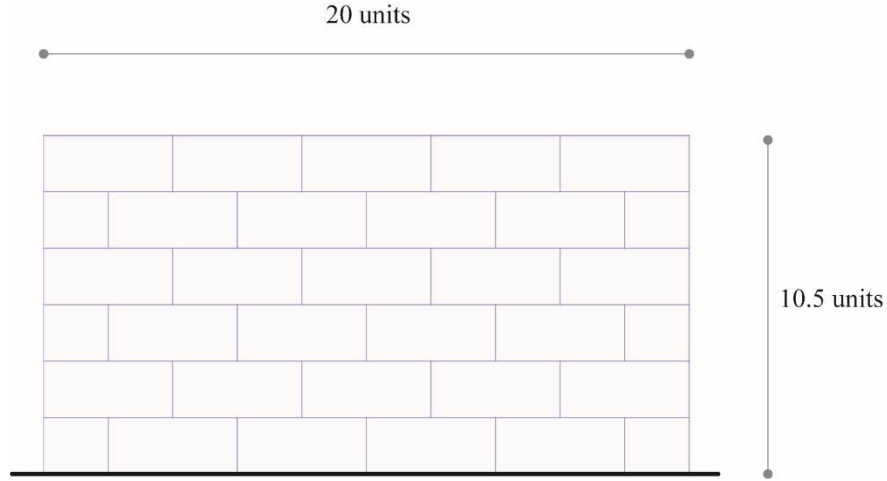


Figure 6: Geometric configuration of the benchmark masonry wall subjected to in-plane horizontal loading [20].

In Table 1, results in terms of upper and lower load multiplier, α_{upp} and α_{low} respectively, as well as crack slope, $\tan \beta$, are reported. Results obtained by using the proposed formulation and the ones obtained by adopting the macro-block formulation proposed in [20], are reported. In the same table, the results arising from the micro-modelling approach discussed in [20] are also summarized. α_{upp} is the upper bound value of the load multiplier which takes into account the friction contribution, while α_{low} .

The results obtained are in good agreement with those available from the macro-block formulation. According to [20], the range obtained the by macro-modelling analysis for the load multiplier always includes that calculated by micro-modelling procedure and a good agreement is also reached for the crack slope. In Figure 7, comparisons in terms of crack slope is reported. The crack line is almost perfectly overlapped with that obtained from both macro and micro modelling developed by Casapulla et al. [20].

Table 1: Predicted load factor and crack slope, Comparisons between the macro and micro-modelling developed by Casapulla et al. [20].

Proposed Model			Macro-block model [20]			Micro-block model [20]		
α_{upp}	α_{low}	$\tan \beta$	α_{upp}	α_{low}	$\tan \beta$	α_{upp}	α_{low}	$\tan \beta$
0.65	0.43	0.515	0.65	0.4221	0.525	0.6393	0.6393	0.7619

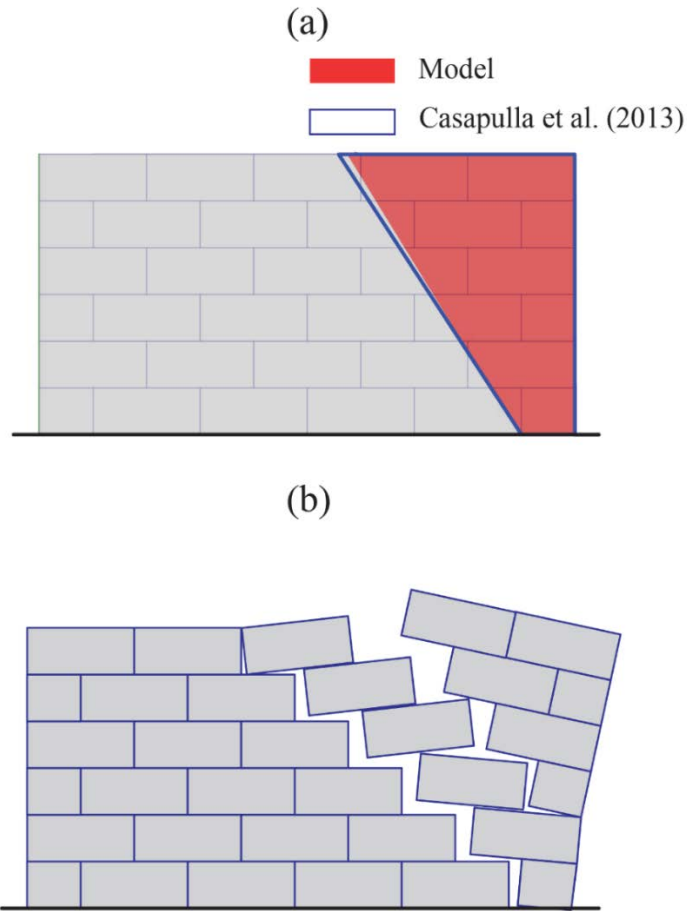


Figure 7: Predicted macro-block geometry, comparisons with macro (a) and micro (b) modelling proposed in [20].

1
2
3
4
5
6
7
8

4.2 Multi-stores masonry building

As shown in Figure 8, the masonry structure considered in this study has two levels and an L shape plan. The floors as well as the roofs are assumed to be made of timber and they are consequently considered to be deformable in their plane. The self-weight for both systems is considered equal to 2 kN/m².

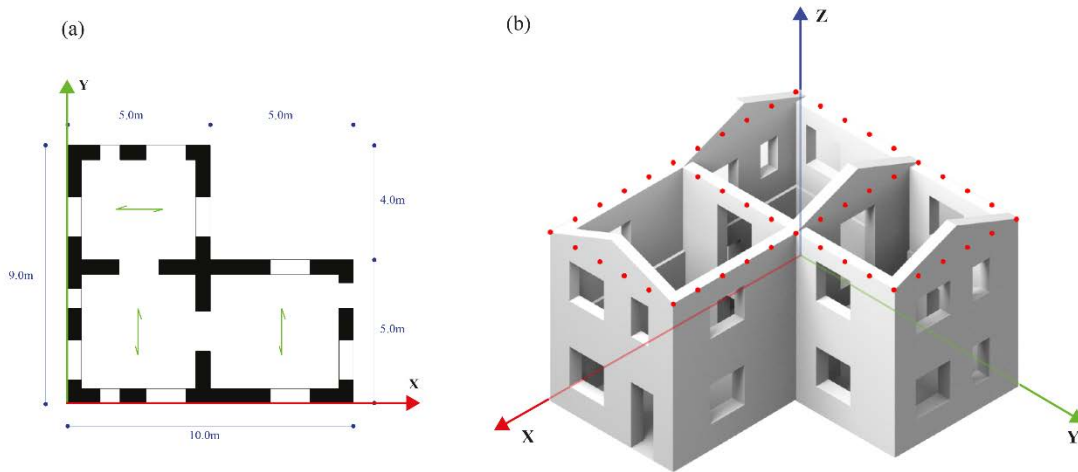


Figure 8: Geometry of the case study. (a) Plan view of the ground floor; (b) 3D view.

Since the proposed procedure would be as general as possible, the geometrical features of the case study are fictitious. The mechanical properties of the CDP utilized in the simulation are taken in agreement with literature [47] as reported in in Table 2 and Table 3.

Table 2: Mechanical properties of the masonry adopted in the simulations.

<i>Material properties</i>	<i>Values</i>
Elastic Modulus	1500 MPa
Poisson ratio	0.2
<i>Dilatation angle</i>	10
<i>Eccentricity</i>	0.1
<i>fb0/fc0</i>	1.16
<i>Kc</i>	0.667
<i>Viscosity Parameter</i>	0.002

Table 3: Compressive and Tensile behaviour of the masonry adopted in the simulations.

Compressive behaviour		Tensile behaviour	
Stress [MPa]	Inelastic strain	Stress [MPa]	Inelastic strain
2.0	0	0.12	0
2.4	0.002	0.0012	0.001
0.2	0.007	0.0012	0.003

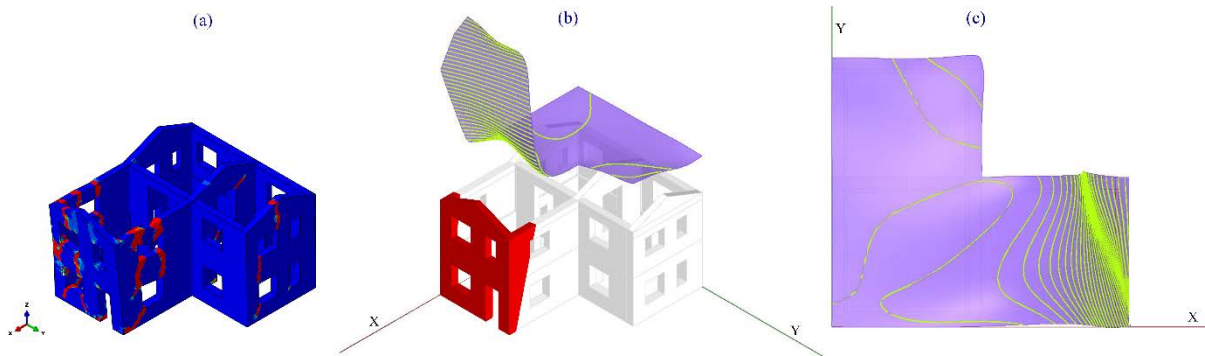
The first step of the push-over methodology requires to apply vertical action including gravity loads. Subsequently, lateral loads consists of forces proportional to the mass, which are separately considered along the axis X and Y, in the positive and negative direction (Figure 8a). In order to perform the procedure described in Section 2 and 3, the horizontal displacements corresponding to 47 control points (red dots in Figure 8) are collected. Although the pushover analysis might be

1 considered along any arbitrary directions, the results of the analysis for the loading configuration
2 along two orthogonal directions as well as positive and negative orientation for the horizontal thrust,
3 are discussed in the following.

5 4.2.1 +X direction

6 Figure 9 shows the CS of the structure at incipient collapse. The geometry of the CS as well as the
7 contour lines allow to visualize the portion of the structure affected by the local mechanism, which
8 consist of the overturning of the façade W5 and portions of the sidewalls W4 and W6.

9 At this stage, the user can set the cylindrical rotation hinge as coincident to the track of the structure
10 intersected by the maximum slope line, which in this case is coincident to the track of W5 (line L1 in
11 Figure 9). As shown in Figure 9a, based on preliminary results, the program detects the macro-block
12 geometry affected by the out-plane mechanism.



13
14 *Figure 9: X direction: (a) damage pattern obtained from the preparatory step (b)CS and identified macro-block (c) Top view CS.*

15
16 At this stage the macro-block geometry, the loads, the frictional coefficient of the masonry
17 (assumed equal to 0.7 [48]) are all set and the constrained optimization problem described in Eq. (5)
18 is solved by adopting both the Octopus ES and Nelder-Mead Optimisation (NMO) Grasshopper
19 components.

20 Figure 10 shows the optimization process, which is based on 20 generations for the ES and 100
21 iterations for NMO. During the first generation, the load factor is equal to 0.43. At each succeeding
22 generation, the result tends to converge to the value which minimises the load multiplier and satisfies
23 the horizontal equilibrium forces, concurrently. Considering a numerical approximation of three
24 digits, the two solving strategies lead to identical results, corresponding to a load multiplier equal to
25 0.354, which drops to 0.164, if frictional effects are not considered.

26

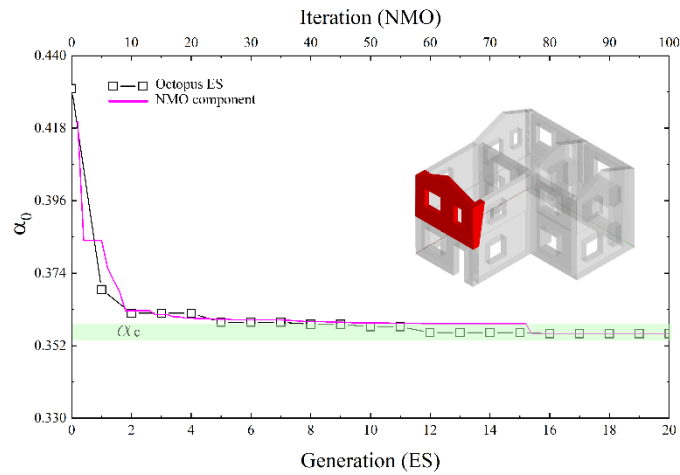


Figure 10: X direction: Load factor vs Generation of the evolutionary solver.

4.2.2 -X direction

The results obtained loading configuration $-X$ are here presented. Figure 11 shows the CS at incipient collapse. The shape of the CS identifies a collapse mechanism which affects the sidewalls W2, W9 and W7, whereas the cylindrical rotation hinge is parallel to W0 and W1.

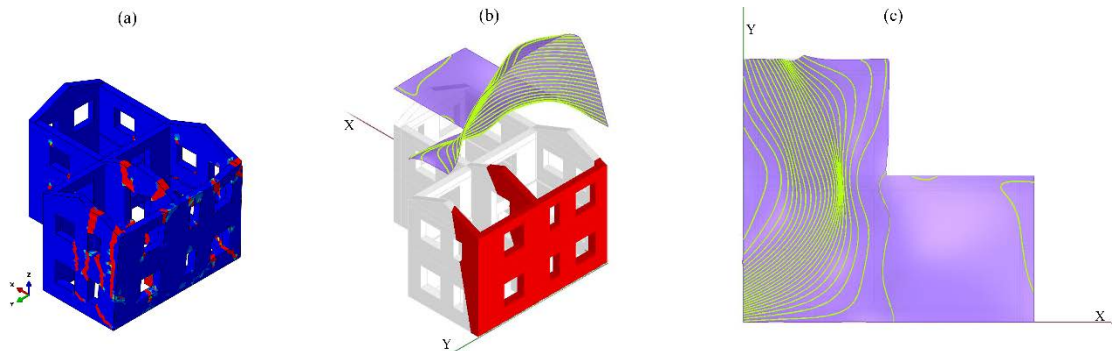
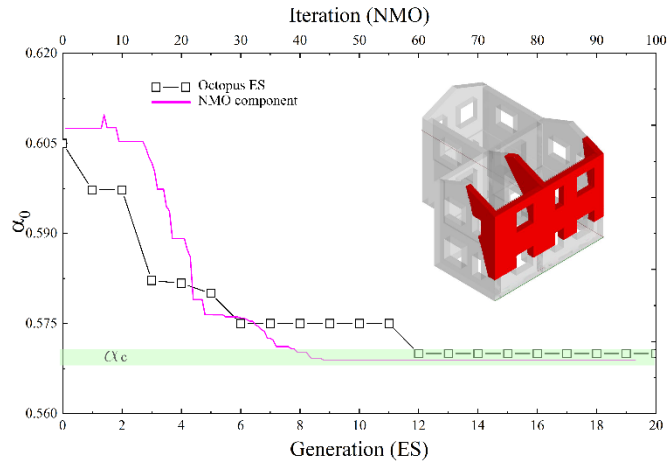


Figure 11: $-X$ direction: (a) damage pattern obtained from the preparatory step (b) CS and identified macro-block (c) Top view CS.

Figure 12 shows the minimum load factor detected at each generation. In this case, the solution is achieved by varying the position (in terms of height) of the cylindrical rotation hinge, which, at convergence, results to be located 1m above the ground level. The macro-block system shown in Figure 12 is employed to compute the load factor within the hypothesis of no friction. In this case the NMO solver converge to a value of the multiplier equal to 0.568, which is slightly lower than the one arising from the ES solution (0.570). If frictional resistance is not considered, the load multiplier results equal to 0.283.



1

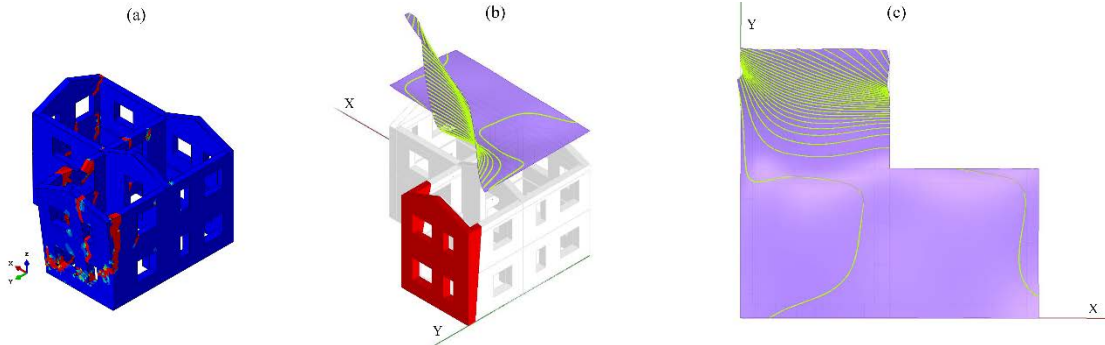
2

Figure 12: -X direction: Load factor vs Generation of the evolutionary solver.

3 4.2.3 +Y direction

4 The load pattern along +Y direction generates a macro-block geometry similar to the one observed
 5 in the case of horizontal forces in the X direction, whilst involving a different portion of the structure
 6 (Figure 13).

7 The maximum values of the CS slope are detected along the wall W3 and W1 (sidewalls),
 8 consequently the wall W2 is affected by the overturning mechanism (Figure 13).



9

10

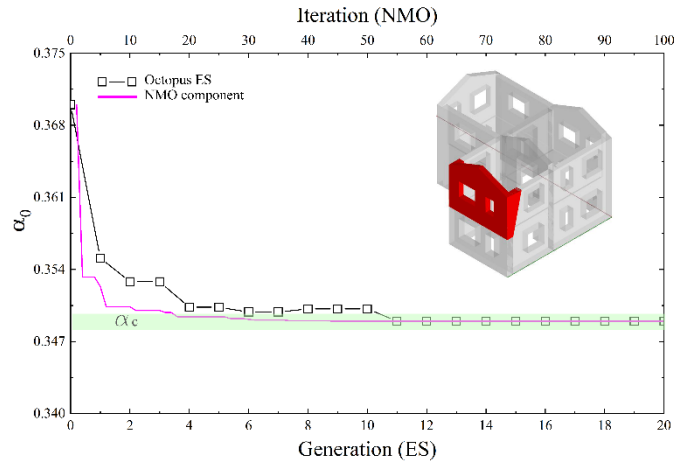
Figure 13: Y direction: (a) damage pattern obtained from the preparatory step (b) CS and identified macro-block (c) Top view CS.

11

12

13

As shown in Figure 14, the evolutionary solver finds the convergence value for a load factor approximately equal to 0.349 by generating the macro block geometry reported in Figure 14. If frictional resistance is not considered, the load multiplier results equal to 0.173.



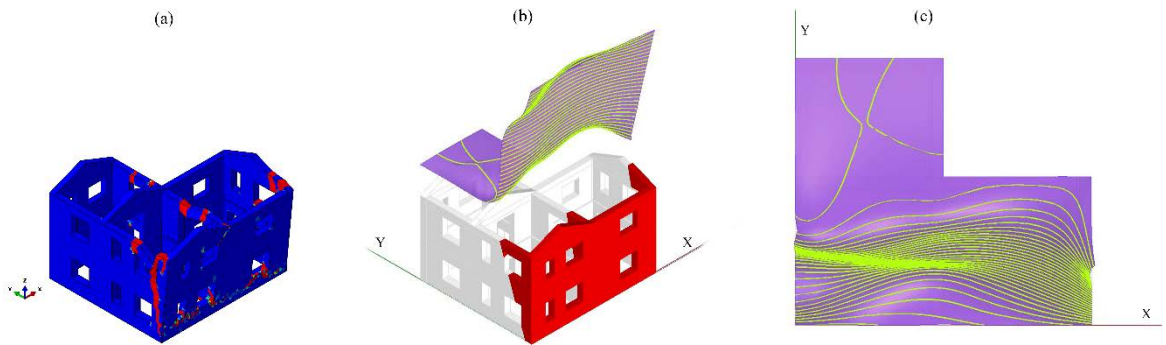
1

2

Figure 14: Y direction: Load factor vs Generation of the evolutionary solver.

3 4.2.4 -Y direction

4 Finally, the load pattern along -Y direction is analysed. As shown in Figure 15, the collapse
 5 mechanism involves three sidewalls i.e. W0, W8 and W5, causing the overturning of the wall W6-
 6 W7.



7

8

Figure 15: -Y direction: (a) damage pattern obtained from the preparatory step (b) CS and identified macro-block (c) Top view CS.

9 The solver converges for a load multiplier 0.373 (Figure 16), which corresponds to the macro-
 10 block geometry depicted in Figure 16. If frictional resistance is not considered, the load multiplier
 11 results equal to 0.198.

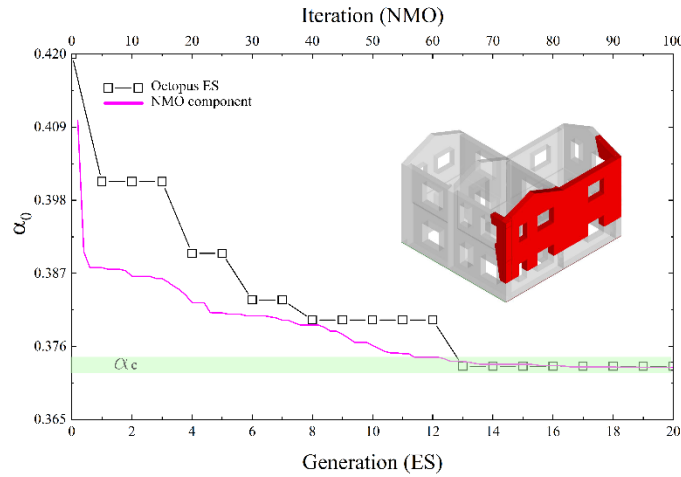


Figure 16: -Y direction: Load factor vs Generation of the evolutionary solver.

1

2

3

4 5. Conclusions

5 In this work, a novel digital procedure for the assessment of masonry structures is proposed.

6 Detailed knowledge of the geometric configuration of historic masonry structures, which
 7 nowadays can be easily achieved using digital survey techniques, is considered the prerequisite of the
 8 assessment procedure. Geometric datasets are employed to generate a detailed 3D model which is
 9 automatically imported into a nonlinear Finite Element (FE) software. Assumptions are made on
 10 mechanical properties of constituent material in absence of detailed information. A pushover analysis,
 11 which is weakly dependent on mechanical parameters in compression, allows to generate a possible
 12 configuration of failure surfaces through the Control Surface Method (CSM), here introduced for the
 13 first time. A further step of analysis embeds an upper bound limit analysis of the problem under the
 14 hypothesis of no-tension capacity for the masonry material. Based on detected failure surfaces,
 15 genetic algorithms are employed to explore a variety of different collapse mechanisms that are
 16 kinematically compatible. The failure mode corresponding to the minimum value of the loads'
 17 multiplier which also satisfy static equilibrium is finally considered the actual collapse mode.

18 The visual approach followed in this work allows to establish relations between the complex
 19 geometries featured by historic masonry structures and their mechanical response. Furthermore, it
 20 allows to immediately visualise the consequences of user's assumptions, allowing to integrate
 21 parametric modelling into decisions-making processes which strongly relies on engineering
 22 judgement

23 The benchmark study presented shows the extensive potential of the method. The CSM allows to
 24 detect the failure modes of the masonry structure considered, demonstrating its suitability to capture
 25 the failure mode of masonry structures with irregular shape. Such methodology overcomes the

1 dependency of the structural methods of analysis on the choice of control point, as a set of control
2 points following a regular grid is a priori selected on the top of the structure.

3 It is worth highlighting that the preliminary non-linear analysis has the role to identify a coarse
4 geometry of the collapse mechanism, rather than to quantify the seismic vulnerability of the structure.
5 Once the geometry of the macro-blocks involved in the mechanism is defined, the detection of the
6 failure modes is refined, and an appropriate distribution of loads is considered in association with the
7 macro-blocks system detected. As the maximum load multiplier causing the failure of the structure is
8 computed using the upper bound theorem of the limit analysis, the result is not affected by the initial
9 choice of mechanical parameters.

10 Future studies will be aimed at generalising the method to different structural typologies and
11 considering the effect of blocks tessellation in the model. Such developments will allow to further
12 reduce the influence of the material parameters choice on the results generated by this procedure.

13 The visual script created during this research is openly available from the University of Dundee
14 data archive at <https://doi.org/10.15132/10000153>, together with a reference manual and a benchmark
15 case study.

16

17 **References**

- 18 1. Bucher, W. and C. Madrid, *Dictionary of building preservation*. 1996: Wiley New York.
- 19 2. Lonetti, P. and R. Maletta, *Dynamic impact analysis of masonry buildings subjected to flood*
20 *actions*. Engineering Structures, 2018. **167**: p. 445-458.
- 21 3. Lourenço, P.B., et al., *Analysis of masonry structures without box behavior*. International
22 *Journal of Architectural Heritage*, 2011. **5**(4-5): p. 369-382.
- 23 4. Fortunato, G., M.F. Funari, and P. Lonetti, *Survey and seismic vulnerability assessment of the*
24 *Baptistry of San Giovanni in Tumba (Italy)*. Journal of Cultural Heritage, 2017. **26**: p. 64-78.
- 25 5. Castellazzi, G., et al., *An innovative numerical modeling strategy for the structural analysis*
26 *of historical monumental buildings*. Engineering Structures, 2017. **132**: p. 229-248.
- 27 6. Korumaz, M., et al., *An integrated Terrestrial Laser Scanner (TLS), Deviation Analysis (DA)*
28 *and Finite Element (FE) approach for health assessment of historical structures. A minaret*
29 *case study*. Engineering Structures, 2017. **153**: p. 224-238.
- 30 7. Dall'Asta, A., et al., *Integrated approach for seismic vulnerability analysis of historic massive*
31 *defensive structures*. Journal of Cultural Heritage, 2018.
- 32 8. Micelli, F. and A. Cascardi, *STRUCTURAL ASSESSMENT AND SEISMIC ANALYSIS OF A*
33 *14TH CENTURY MASONRY TOWER*. Engineering Failure Analysis, 2019: p. 104198.
- 34 9. D'Altri, A.M., et al., *Modeling Strategies for the Computational Analysis of Unreinforced*
35 *Masonry Structures: Review and Classification*. Archives of Computational Methods in
36 Engineering, 2019.
- 37 10. Silva, L.C., et al., *Seismic Structural Assessment of the Christchurch Catholic Basilica, New*
38 *Zealand*. Structures, 2018. **15**: p. 115-130.
- 39 11. Valente, M. and G. Milani, *Damage assessment and collapse investigation of three historical*
40 *masonry palaces under seismic actions*. Engineering Failure Analysis, 2019. **98**: p. 10-37.
- 41 12. Heyman, J., *The stone skeleton*. International Journal of solids and structures, 1966. **2**(2): p.
42 249-279.

- 1 13. Giuffrè, A. and C. Carocci, *Statica e dinamica delle costruzioni murarie storiche*. Atti del
2 Convegno internazionale CNR “Le pietre da costruzione: il tufo calcareo e la pietra leccese”.
3 Mario Adda Editore, Bari, 1993: p. 539-598.
- 4 14. Angelillo, M., *Mechanics of masonry structures*. 2014: Springer.
- 5 15. D'Ayala, D.F. and E. Tomasoni, *Three-dimensional analysis of masonry vaults using limit*
6 *state analysis with finite friction*. International Journal of Architectural Heritage, 2011. **5**(2):
7 p. 140-171.
- 8 16. Casapulla, C., et al., *3D macro and micro-block models for limit analysis of out-of-plane*
9 *loaded masonry walls with non-associative Coulomb friction*. Meccanica, 2014. **49**(7): p.
10 1653-1678.
- 11 17. D'Ayala, D., *Assessing the seismic vulnerability of masonry buildings*, in *Handbook of*
12 *seismic risk analysis and management of civil infrastructure systems*. 2013, Elsevier. p. 334-
13 365.
- 14 18. D'Altri, A., et al., *A review of numerical models for masonry structures*. Numerical Modeling
15 of Masonry and Historical Structures: From Theory to Application, 2019: p. 1.
- 16 19. Fortunato, A., et al., *Limit analysis of masonry structures with free discontinuities*. Meccanica,
17 2018. **53**(7): p. 1793-1802.
- 18 20. Casapulla, C., et al., *A macro-block model for in-plane loaded masonry walls with non-*
19 *associative Coulomb friction*. Meccanica, 2013. **48**(9): p. 2107-2126.
- 20 21. Chiozzi, A., et al., *A fast and general upper-bound limit analysis approach for out-of-plane*
21 *loaded masonry walls*. Meccanica, 2018. **53**(7): p. 1875-1898.
- 22 22. Chiozzi, A., G. Milani, and A. Tralli, *A Genetic Algorithm NURBS-based new approach for*
23 *fast kinematic limit analysis of masonry vaults*. Computers & Structures, 2017. **182**: p. 187-
24 204.
- 25 23. Giresini, L., *Energy-based method for identifying vulnerable macro-elements in historic*
26 *masonry churches*. Bulletin of Earthquake Engineering, 2016. **14**(3): p. 919-942.
- 27 24. Cundari, G.A., G. Milani, and G. Failla, *Seismic vulnerability evaluation of historical*
28 *masonry churches: Proposal for a general and comprehensive numerical approach to cross-*
29 *check results*. Engineering Failure Analysis, 2017. **82**: p. 208-228.
- 30 25. Betti, M. and L. Galano, *Seismic analysis of historic masonry buildings: the vicarious palace*
31 *in Pescia (Italy)*. Buildings, 2012. **2**(2): p. 63-82.
- 32 26. Mele, E., A. De Luca, and A. Giordano, *Modelling and analysis of a basilica under*
33 *earthquake loading*. Journal of Cultural Heritage, 2003. **4**(4): p. 355-367.
- 34 27. Brandonisio, G., et al. *Seismic safety of basilica churches: Analysis of ten case studies*. 2008.
- 35 28. Mendes, N. and P.B. Lourenço, *Chapter 4 - Seismic assessment of historic masonry*
36 *structures: out-of-plane effects*, in *Numerical Modeling of Masonry and Historical Structures*,
37 B. Ghiassi and G. Milani, Editors. 2019, Woodhead Publishing. p. 141-162.
- 38 29. Foti, D. and V. Vacca, *Rocking of multiblock stone classical columns*. WIT Transactions on
39 the Built Environment, 2017. **172**.
- 40 30. Foti, D., V. Vacca, and S. Ivorra. *Influence of connections in the seismic behaviour of trilithic*
41 *large blocks masonry structures*. in *Brick and Block Masonry: Trends, Innovations and*
42 *Challenges - Proceedings of the 16th International Brick and Block Masonry Conference,*
43 *IBMAC 2016*. 2016.
- 44 31. *Eurocode 6: Design of masonry structures - Part 1-1: General rules for reinforced and*
45 *unreinforced masonry structures*. 1996.
- 46 32. *Ministero dei Lavori Pubblici, Decreto Ministeriale 17/01/2018, Norme tecniche per le*
47 *costruzioni*. 2008.
- 48 33. *Linee Guida per la valutazione e riduzione del rischio sismico del patrimonio culturale*
49 *allineate alle nuove Norme tecniche per le costruzioni* 2010.
- 50 34. Fajfar, P., *A nonlinear analysis method for performance-based seismic design*. Earthquake
51 spectra, 2000. **16**(3): p. 573-592.

- 1 35. Clementi, F., et al., *Assessment of seismic behaviour of heritage masonry buildings using*
2 *numerical modelling*. Journal of Building Engineering, 2016. **8**: p. 29-47.
- 3 36. Casolo, S. and G. Uva, *Nonlinear analysis of out-of-plane masonry façades: full dynamic*
4 *versus pushover methods by rigid body and spring model*. Earthquake Engineering &
5 Structural Dynamics, 2013. **42**(4): p. 499-521.
- 6 37. Foti, D., *A new experimental approach to the pushover analysis of masonry buildings*.
7 Computers and Structures, 2015. **147**: p. 165-171.
- 8 38. Olivito, R.S. and S. Porzio, *A new multi-control-point pushover methodology for the seismic*
9 *assessment of historic masonry buildings*. Journal of Building Engineering, 2019. **26**.
- 10 39. Olivito, R.S., et al. *A numerical-geometrical methodology to represent out-of-plane*
11 *mechanisms of unreinforced masonry structures by using pushover analysis*. 2019. National
12 Technical University of Athens.
- 13 40. Casapulla, C., et al., *Corner failure in masonry buildings: An updated macro-modeling*
14 *approach with frictional resistances*. European Journal of Mechanics, A/Solids, 2018. **70**: p.
15 213-225.
- 16 41. Rutten, D., *Galapagos: On the logic and limitations of generic solvers*. Architectural Design,
17 2013. **83**(2): p. 132-135.
- 18 42. Lubliner, J., et al., *A plastic-damage model for concrete*. International Journal of solids and
19 structures, 1989. **25**(3): p. 299-326.
- 20 43. Valente, M. and G. Milani, *Non-linear dynamic and static analyses on eight historical*
21 *masonry towers in the North-East of Italy*. Engineering Structures, 2016. **114**: p. 241-270.
- 22 44. Castellazzi, G., et al., *An innovative numerical modeling strategy for the structural analysis*
23 *of historical monumental buildings*. Engineering Structures, 2017. **132**: p. 229-248.
- 24 45. Malena, M., et al., *Collapse mechanism analysis of historic masonry structures subjected to*
25 *lateral loads: A comparison between continuous and discrete models*. Computers and
26 Structures, 2019. **220**: p. 14-31.
- 27 46. Gregson, S., *Nelder-Mead Optimisation (EOC)*,
28 [https://www.eocengineers.com/en/news/digital-design-group-tackles-classic-engineering-](https://www.eocengineers.com/en/news/digital-design-group-tackles-classic-engineering-problem)
29 [problem](https://www.eocengineers.com/en/news/digital-design-group-tackles-classic-engineering-problem) 2018.
- 30 47. D'Altri, A.M., et al., *Seismic-induced damage in historical masonry vaults: A case-study in*
31 *the 2012 Emilia earthquake-stricken area*. Journal of Building Engineering, 2017. **13**: p. 224-
32 243.
- 33 48. Marino, M., et al. *Experimental data of friction coefficient for some types of masonry and its*
34 *correlation with an Index of Quality Masonry (IQM)*. in *Proceedings 2nd European*
35 *Conference on Earthquake Engineering and Seismology, Istanbul*. 2014.

36

1	List of Figures	
2	Figure 1: Control Surface detected at last loading increment of the non-linear static analysis.....	6
3	Figure 2: Slope map representation and local analysis performed on single sidewalls.....	7
4	Figure 3: (a) Geometry of the macro-block obtained from the visual program; (b) Displacement map	
5	arising from the non-linear static analysis at the last load increment.	8
6	Figure 4: Evolutionary Solver: Genes definition, generations representation and graphical	
7	representation of the genomes.....	9
8	Figure 5: Schematic representation of the proposed procedure.....	10
9	Figure 6: Geometric configuration of the benchmark masonry wall subjected to in-plane horizontal	
10	loading [20].	14
11	Figure 7: Predicted macro-block geometry, comparisons with macro (a) and micro (b) modelling	
12	proposed in [20].	15
13	Figure 8: Geometry of the case study. (a) Plan view of the ground floor; (b) 3D view.	16
14	Figure 9: X direction: (a) damage pattern obtained from the preparatory step (b) CS and identified	
15	macro-block (c) Top view CS.	17
16	Figure 10: X direction: Load factor vs Generation of the evolutionary solver.....	18
17	Figure 11: -X direction: (a) damage pattern obtained from the preparatory step (b) CS and identified	
18	macro-block (c) Top view CS.	18
19	Figure 12: -X direction: Load factor vs Generation of the evolutionary solver.	19
20	Figure 13: Y direction: (a) damage pattern obtained from the preparatory step (b) CS and identified	
21	macro-block (c) Top view CS.	19
22	Figure 14: Y direction: Load factor vs Generation of the evolutionary solver.....	20
23	Figure 15: -Y direction: (a) damage pattern obtained from the preparatory step (b) CS and identified	
24	macro-block (c) Top view CS.	20
25	Figure 16: -Y direction: Load factor vs Generation of the evolutionary solver.	21

26

27

28 **List of Tables**

29	Table 1: Predicted load factor and crack slope, Comparisons between the macro and micro-	
30	modelling developed by Casapulla et al. [19].....	14
31	Table 2: Mechanical properties of the masonry adopted in the simulations.....	16
32	Table 3: Compressive and Tensile behaviour of the masonry adopted in the simulations.....	16

33